Fractionation in a Phase-Separated Polydisperse Polymer Mixture

A. van Heukelum,*,† G. T. Barkema,† M. W. Edelman,‡,§ E. van der Linden,§ E. H. A. de Hoog,‡,⊥ and R. H. Tromp‡,⊥

Institute for Theoretical Physics, Utrecht University, Leuvenlaan 4, 3584 CE Utrecht, The Netherlands; Wageningen Centre for Food Sciences, PO Box 557, Diedenweg 20, 6700 AN Wageningen, The Netherlands; Food Physics Group, Department of Agrotechnology and Nutrition Sciences, Wageningen University, Bomenweg 2, 6703 HD Wageningen, The Netherlands; and NIZO Food Research, Kernhemseweg 2, P.O. Box 20, 6710 BA Ede, The Netherlands

Received October 14, 2002; Revised Manuscript Received June 11, 2003

ABSTRACT: If a solution of polydisperse A- and B-polymers undergoes phase separation, the molar mass distribution of the A-polymers in the A-rich phase becomes different from that in the B-rich phase. This phenomenon is known as fractionation. Here, we compare experimental results on fractionation with Flory−Huggins theory and computer simulations. We study the degree of fractionation $f(m) \equiv \rho_{\text{A in B}}(m)/\rho_{\text{A in A}}(m)$, in which $\rho_{\text{A in A}}(m)$ is the density of A-polymers with molar mass m in the A-rich phase and $\rho_{\text{A in B}}(m)$ that of A-polymers in the B-rich phase. We find that $f(m)$ obeys the simple scaling $f(m) \sim \exp(-km)$, where k is a temperature-dependent constant.

I. Introduction

Our current theoretical understanding of phase separation of mixtures is based on the pioneering work of Flory[1,2] and Huggins[3,4] as well as Scott,[5−7] who presented a mean-field approximation to the free energy of binary mixtures. Several groups[8−13] have studied the dynamics of multicomponent systems and in particular nucleation and spinodal decomposition, based on the Flory−Huggins free energy expression. With small adjustments to the Flory−Huggins theory, liquid−liquid phase separation of polymeric systems has also been investigated.[14−24] Some of these studies have also considered polydisperse binary and quasi-binary polymer mixtures.[16,20,23,24] Recently, an excellent review paper on the current theoretical understanding of phase equilibria in polydisperse systems has appeared.[25] However, to the best of our knowledge, no theoretical results are reported on the topic of our work—the equilibrium molar mass distributions of the polymers in a phase-separated polydisperse binary polymer mixture.

Experiments on polymer mixtures have been reported by several groups, including those in refs 26−31. These experiments determined under which conditions phase separation sets in and dynamical properties of the phase-separation process; properties of each of the separated phases are not discussed. Recently, some of us have studied the composition of the separated phases of aqueous mixtures of gelatin and dextran.[32] In section II we will summarize the main findings of this latter paper.

Computer simulations of lattice models for polymeric systems have been performed, based on a model of Verdier and Stockmayer,[33−37] on self-avoiding walks,[38,39] and on the bond fluctuation model (BFM).[22,40−42] In this work, we use a different lattice polymer model, which is described in section III. It has been studied with Flory−Huggins theory in section IV and with computer simulations in section V. We conclude with a section in which we compare the results of the experiments, the Flory−Huggins theory, and the computer simulations with respect to the composition of the phases of the separated polymer mixture.

II. Experimental Part

In earlier experimental work, we studied the effect of phase separation on the molar mass distributions of aqueous mixtures of gelatin and dextran.[32] These two biopolymers are both polydisperse with respect to their molar mass. Aqueous mixtures of gelatin and dextran were made to phase separate. After full phase separation was established, samples of both phases were analyzed with use of size exclusion chromatography and multiangle laser light scattering (SEC-MALLS) to determine the molar mass distribution of both components in coexisting phases. Full phase separation of aqueous mixtures of gelatin and dextran results in a gelatin-rich and a dextran-rich phase. However, both phases contain both polymers.[43] Figure 1 shows the effect of phase separation on the molar mass distribution of gelatin (left) and dextran (right). It turns out that the minority type of molecules in each phase consist of the small molar mass part of the distribution.

To quantify this observation, we determine the *degree of fractionation*:

$$f^x(m) \equiv c^x_{\text{poor}}(m)/c^x_{\text{rich}}(m) \tag{1}$$

in which $c^x_{\text{poor}}(m)$ and $c^x_{\text{rich}}(m)$ are the concentrations of component x (gelatin or dextran) with a degree of polymerization m in the depleted (poor) and the enriched (rich) phase, respectively. The value $m = 1$ corresponds to a monomer. For gelatin, the monomer mass is taken 90 Da (the average mass of an amino acid in the gelatin used) and for dextran 162 Da (the mass of a glucose repeating unit).

If we plot $f^x(m)$ vs the degree of polymerization, it turns out that the fractionation shows exponential behavior for both gelatin and dextran (see Figure 2).

III. Lattice Model

The particular lattice polymer model that we use describes a polymer of length L as a self-avoiding walk on a face-centered-cubic (fcc) lattice, with the exception

† Utrecht University.
‡ Wageningen Centre for Food Sciences.
§ Wageningen University.
⊥ NIZO Food Research.

10.1021/ma025736q CCC: $25.00
Published on Web 07/30/2003

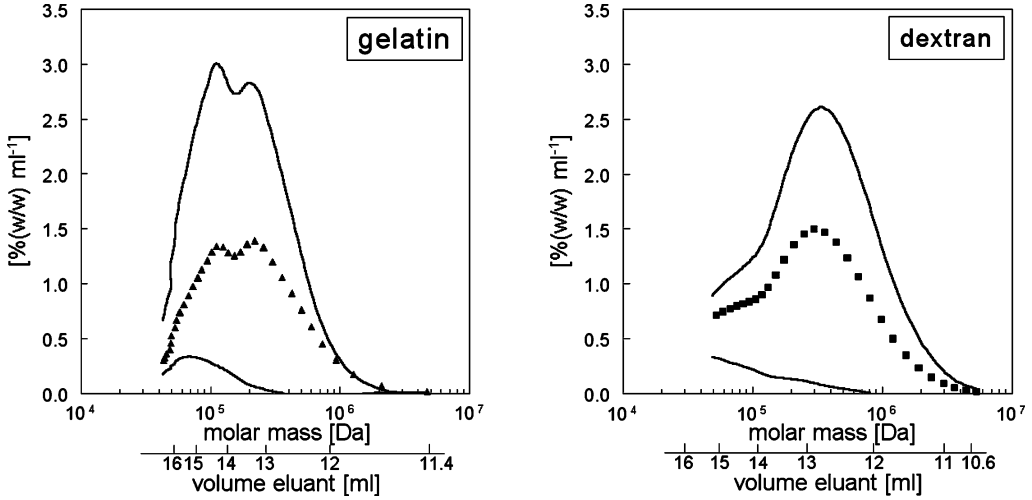

Figure 1. Effect of phase separation on the molar mass distributions of gelatin and dextran in coexisting phases after phase separation of a mixture containing 5% (w/w) gelatin and 5% (w/w) dextran, at 60 °C. Left: gelatin (M_w = 184 kDa); right: dextran (M_w = 299 kDa). The upper lines show the concentrations in the rich phase and the lower lines in the poor phase; the dots show the concentrations before phase separation.

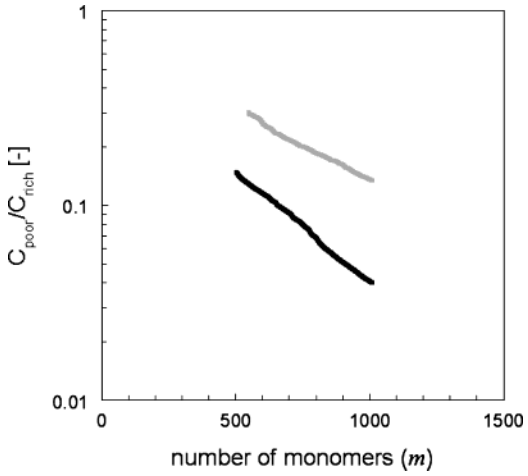

Figure 2. Degree of fractionation $f(m)$ as a function of polymer length (number of monomers) for a sample containing 5% (w/w) gelatin and 5% (w/w) dextran at T = 60 °C. The gray and black lines correspond to gelatin and dextran, respectively.

that monomers which are adjacent in the chain may occupy the same lattice site. The set of lattice sites occupied by the polymer is called the *tube*, and the difference between L and the length of the tube is called *stored length*. Monomers belonging to different polymers are never allowed to reside on the same lattice site.

This particular lattice polymer lends itself extremely well for computer simulations. The polymers diffuse by two different kinds of Monte Carlo mechanisms. The first mechanism is that of reptation along a chain: if for a given monomer one of its adjacent monomers is located on the same lattice site, while its other adjacent monomer is located on a nearest-neighbor lattice site, it can move to that lattice site. As we will show below, interactions can be defined such that this kind of move does not change the total energy. This allows a highly efficient implementation of those moves using multispin coding techniques.[44] A contracted end monomer, on the same lattice site as its neighbor in the chain, can move to a randomly chosen neighboring empty site, and an extended end monomer can move to the lattice site that contains its neighbor in the chain.

The second mechanism in our simulations corresponds to sideways movement of the polymer. Proposed moves for this mechanism are single-lattice-site displacements of a single monomer that leave the polymer configuration valid. These moves may change the tube length of the polymer by adding or removing stored length.

We have chosen a fcc lattice instead of the more common simple-cubic lattice because the latter would severely restrict the freedom in sideways movement. The effective rates of reptation moves and sideways moves depend on the amount of stored length in the polymers and are highest if 50% of the bonds are stored length. We have chosen a ratio of $z/2$ between attempt rates for moves that increase or decrease the tube length, where z = 12 is the coordination number of the fcc lattice. This is incorporated by a difference in entropy related with stored length of $\ln(z/2)$.

The phase separation of the two polymer types is induced by a short-range repulsive interaction between the different types of polymers. The interaction energy between two nearest-neighbor lattice sites is $\epsilon_{AB} = J$ if the two lattice sites are occupied with different types of monomers. The other polymer−polymer interactions (ϵ_{AA} and ϵ_{BB}), polymer−solvent interactions (ϵ_{A0} and ϵ_{B0}), and the solvent−solvent interactions (ϵ_{00}) are set to zero. Note that the strength of the interaction is independent of the number of monomers residing on the lattice sites.

To incorporate the change in total energy due to a move, we apply a Metropolis accept−reject procedure.[45] If the change in total energy ΔE is negative (i.e., the energy decreases), the proposed move is always accepted; otherwise, the acceptance probability is equal to $P_{accept} = \exp(-\Delta E/(k_B T))$, in which k_B is the Boltzmann constant and T the temperature.

Our goal to implement reptation dynamics with high computational efficiency explains why in our model we do not apply an excluded-volume constraint to adjacent monomers in the chain as well as why we choose interaction strengths between nearest-neighbor lattice sites independent of the number of monomers that occupy the lattice sites. In our implementation, reptation moves take 2 ns CPU time[49] on average, end monomer moves take 90 ns on average, and sideways moves take 90 ns on average. Reptation moves and end monomer moves are attempted at a 30 times higher rate than the sideways moves. On average, a move takes

about 3 ns for a polymer distribution with an average length of 165 monomers, which we used for our simulations.

While the two mechanisms above reflect realistic dynamics of polymer mixtures, we also used a third mechanism that is highly artificial. In this mechanism, the proposed move is to change the type of a randomly chosen single polymer from type A to B or vice versa. This proposed move is then accepted or rejected according to the Metropolis algorithm. This mechanism does not alter equilibrium properties but should not be used if dynamical properties are studied.

Each of these three mechanisms is implemented in a way that ensures detailed balance, and the combination of these three mechanisms ensures a complete exploration of phase space; i.e., ergodicity is obtained. The combination of detailed balance and ergodicity guarantees that eventually configurations are generated according to the Boltzmann distribution.

IV. Flory−Huggins Theory

We present here Flory−Huggins theory applied to our particular lattice model of polydisperse polymer mixtures. First, we introduce the theory for a monodisperse symmetric mixture and then extend it to general polydisperse systems. The resulting expression for the free energy is minimized numerically for the molar mass distributions of the initial constituents of the polymer solutions used in the experiments and those used in our computer simulations.

For a binary polymer mixture with a repulsive interaction between the two types, phase separation is energetically favorable but entropically unfavorable. The simplest theory of the phase transition in such systems originates from Flory and Huggins. Below, we present it first for a monodisperse symmetric mixture, but we do not assume that the polymer system is large. The entropy of mixing is the logarithm of the number of ways one can split the set of polymers into a phase with p polymers of type A and q polymers of type B and another phase with q polymers of type A and p polymers of type B. The entropy of mixing for either phase is

$$S = k_B \ln \frac{(p+q)!}{p!\,q!} \tag{2}$$

which has a maximum at $p = q$, i.e., for two equal phases. Flory and Huggins were only interested in the limit where p and q are both very large and used Stirling's approximation to arrive at the well-known result

$$S_{FH} = -k_B p \ln \frac{p}{p+q} - k_B q \ln \frac{q}{p+q}$$

We assume that the polymers are randomly distributed throughout the system and that effects of the chain structure on the energy of the system can be described by introducing an effective coordination number z_{eff}, instead of the lattice coordination number z. The total energy of the system, in this mean-field approximation, is proportional to the number of nearest-neighbor lattice sites occupied by different type monomers, with a proportionality constant J. The system contains V lattice sites. In a single phase, $(\rho_s/\rho_m)pL$ sites are occupied with one type of monomers and $(\rho_s/\rho_m)qL$ sites are occupied with the other type, where ρ_s and ρ_m are the density of occupied lattice sites and the monomer density, respectively. Note that ρ_s and ρ_m are not equal due to the possibility of multiple adjacent monomers occupying a single lattice site. With these assumptions, the polymers of type A have $(\rho_s/\rho_m)pLz_{eff}$ interactions with neighboring lattice sites, but only the fraction $(\rho_s/\rho_m)qL/V$ is occupied by monomers of type B. The energy is

$$E = \frac{\alpha J z}{V} L^2 pq \tag{3}$$

with $\alpha = (\rho_s/\rho_m)^2(z_{eff}/z)$.

The physical system in equilibrium, at constant pressure, will minimize the Gibbs free energy for a system, which is almost equivalent to minimizing the Helmholtz free energy, for constant volume, because the system is almost incompressible. The Flory−Huggins theory is based on the mean-field free energy expression for a system with a constant number of particles and a constant volume. The Helmholtz free energy of a single phase, $F = E - TS$, is given by

$$F = \frac{\alpha J z}{V} L^2 pq - k_B T \ln \frac{(p+q)!}{p!\,q!} \tag{4}$$

The free energy has a minimum at $H_p - cp = H_q - cq$, where $H_n = \sum_{i=1}^{n} i^{-1}$ is the nth harmonic number and $c = (\alpha J z/V)(L^2/k_B T)$ is the total effective interaction between the polymers. The harmonic numbers behave like $H_n \approx \ln n$ for large n, and the continuous version goes to zero for small n. Indeed, if we may assume large numbers of polymers for both polymer types, we can use $H_n \approx \ln n + \gamma$, and we arrive at the equation $\ln p - cp = \ln q - cq$, which is precisely the same result as if one used the Flory−Huggins free energy instead of eq 2. The constant $\gamma = 0.577216...$ is known as Euler's constant.

A general phase-separated polydisperse polymer mixture can be described as a set of boxes $\{B\}$, containing polymers from a set of different species (types of polymers) $\{S\}$, and a set of different lengths $\{L\}$. The expression for the entropy becomes

$$S = k_B \ln \prod_{s\in\{S\}} \prod_{l\in\{L\}} \frac{(\sum_{b\in\{B\}} n_{slb})!}{\prod_{b\in\{B\}} n_{slb}!} \tag{5}$$

where n_{slb} is the number of polymers of species s and length l present in box b. Maximum entropy is reached if all boxes have equal volume and contain the same amount of polymers of each type and length. We can rewrite the logarithm of the product as a sum of logarithms and, in the limit where all $n_{slb} \gg 1$, use Stirling's approximation to avoid the factorials:

$$S_{FH} = -k_B \sum_{s\in\{S\}} \sum_{l\in\{L\}} \sum_{b\in\{B\}} n_{slb} \ln n_{slb} + \text{const} \tag{6}$$

The energy of mixing is again considered by a mean-field approximation:

$$E = \frac{\alpha z}{2} \sum_{b\in\{B\}} \frac{1}{V_b} \sum_{l\in\{L\}} \sum_{l'\in\{L\}} \sum_{s\in\{S\}} \sum_{s'\in\{S\}} (\epsilon_{ss'} - \epsilon_{0s} + \epsilon_{00}) n_{slb} l n_{s'l'b} l' + \text{const} \tag{7}$$

where V_b is the number of lattice sites in box b.

We now turn to the polydisperse case with two components A and B, with only interactions between nearest-neighbor sites occupied by different types, i.e., $\epsilon_{AB} = J \neq 0$. It is convenient to change notation: we denote the number of A-polymers of length L_i in box b with p_i^b, and the number of B-polymers of length L_i in box b with q_i^b. The free energy then becomes

$$F = \sum_b \frac{\alpha J z}{V_b}\left(\sum_i p_i^b L_i\right)\left(\sum_i q_i^b L_i\right) + k_B T \sum_{b,i} p_i^b \ln p_i^b + k_B T \sum_{b,i} q_i^b \ln q_i^b + \text{const} \quad (8)$$

Again, V_b is the volume of box b. Given a starting distribution, we can minimize this free energy under the constraints that the total number of A- and B-polymers of each length is constant and that the total volume $V = V_1 + V_2$ is constant.

We created the density $\rho(m)$ of polymers containing m monomers from the experimental molar mass distribution $c(m \cdot m_0)$ in which m_0 is the mass of a monomer (90 Da for gelatin, 162 Da for dextran) as follows. First, we approximated the experimental molar mass distribution (Figure 1) by the sum of Gaussians with mean value $\ln(a_i)$ and width σ_i (four Gaussians for gelatin, three for dextran):

$$\rho(m) \approx \sum_i k_i \exp\left(-\frac{[\ln(m) - \ln(a_i)]^2}{2\sigma_i^2}\right) \quad (9)$$

Next, the sum of these two length distributions was divided into 100 bins containing the same number of polymers. Each bin is then represented by a monodisperse population with the average length and appropriately chosen fractions of dextran and gelatin.

Using the Flory−Huggins expression, we minimized the free energy for a configuration in two boxes. We expect that the degree of fractionation is exponential in the length of the polymers, i.e., $f(m) \sim (-km)$, and therefore plot

$$k(m) \equiv -m^{-1} \ln f(m) \quad (10)$$

as a function of temperature (see Figure 3). As expected, measurements for different polymer lengths fall on top of each other in this figure, showing that the degree of fractionation $f(m)$ changes exponentially with the polymer length. The figure shows that the two boxes contain equal phases above $T/\alpha J = 4.80 \times 10^3$ and different phases below that value, one rich in gelatin and the other rich in dextran. In mean-field theory, we expect that the critical exponent for phase separation is $\beta_{FH} = {}^1/_2$. In the inset of the figure we plot $|k(m)|^{1/\beta_{FH}}$ in the critical regime, which indeed shows linear behavior up to the critical temperature.

Our computer simulations are limited to identical polydispersity for the two types of polymers. We fitted a single Gaussian to the average of the length distributions of gelatin and dextran and then proceeded as above to obtain a population of 45 different lengths. For computational efficiency, the average polymer length within the simulations was 165 monomers. The molar mass of this distribution was $M_w = 214$ monomers, as compared to a few thousand in the experiments. Also, for the length distribution used in the simulations, we applied Flory−Huggins theory. Figure 4 shows the resulting $k(m) = -m^{-1} \ln f(m)$ as a function of temperature. Well below the critical temperature, the short polymers deviate from the relation $f(m) \sim (-km)$, toward a higher degree of fractionation. This deviation decreases with increasing polymer lengths and disappears completely if Stirling's approximation were used.

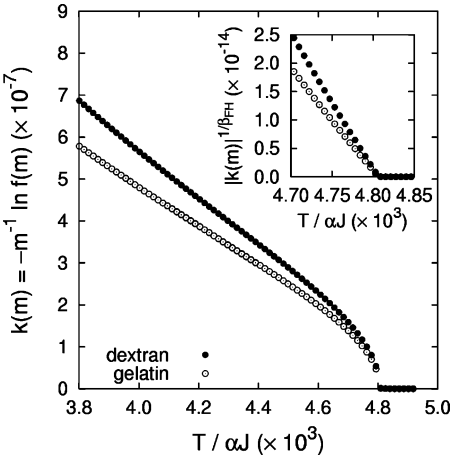

Figure 3. Flory−Huggins results for $k(m) \equiv -m^{-1} \ln f(m)$ as a function of dimensionless temperature for dextran (upper points) and gelatin (lower points). The curves for all polymer lengths m coincide, showing that the degree of fractionation increases exponentially with length. The inset shows that $|k(m)|^{1/\beta_{FH}}$ decreases linearly with temperature, up to its critical value.

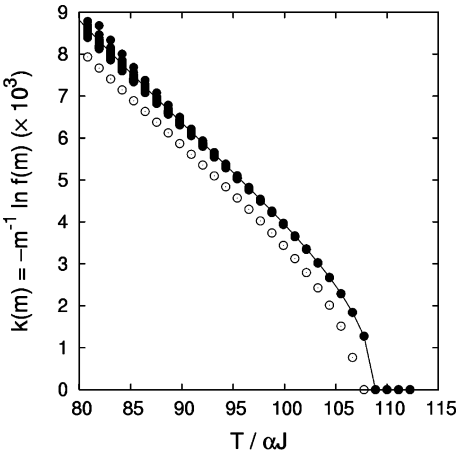

Figure 4. Flory−Huggins results for $k(m) = -m^{-1} \ln f(m)$ as a function of dimensionless temperature for the polymer length distributions used in the computer simulations, with and without Stirling's approximation (lower and upper points, respectively).

V. Computer Simulations

We performed computer simulations of the model, with polydispersity as described above, containing 5400 polymers in total, on a fcc lattice with 1 728 000 sites. All simulations start with a system generated and equilibrated without nearest-neighbor interactions, i.e., at infinite temperature. We use the three types of moves as described in section III to bring the system in equilibrium at the selected temperature. We keep track of the number of polymers of type A and B for each polymer length. The averages of these data are used to determine the phase separation temperature and the fractionation of the different polymer lengths.

With decreasing temperature, the binary polymer mixture separates into two equivalent phases, and the

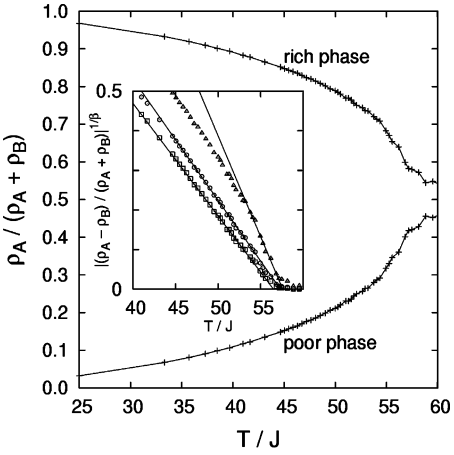

Figure 5. Relative weight $\rho_A/(\rho_A + \rho_B)$ of A-polymers in their rich (upper curve) and poor phase (lower curve) as a function of temperature. The inset shows $|(\rho_A - \rho_B)/(\rho_A + \rho_B)|^{1/\beta}$, which is expected to decrease linearly to zero at the critical temperature. We plotted the data with three values for the exponent: $\beta = 0.3269$ (squares) as in the 3D Ising model, the Fisher-renormalized value $\beta = 0.37$ (circles), and the mean-field value $\beta = 0.5$ (triangles). The straight lines are fits by the eye, fitting the critical temperature (zero-crossing) and amplitude (slope). Our data are well described with $\beta = 0.3269$ or $\beta = 0.37$ but are incompatible with the mean-field value $\beta = 0.5$. Above the critical temperature, the rich phase and poor phase are still distinguishable due to the finite size of the box.

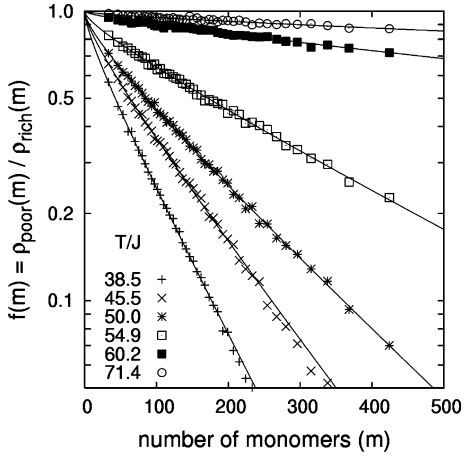

Figure 6. Degree of fractionation $f(m)$, as a function of polymer length, measured in the number of monomers m, for temperatures $T/J = 38.5$, 45.5, 50.0, 54.9, 60.2, and 71.4. Lines are fits to the function $f'(m) = \exp(-km - k_2\sqrt{m})$.

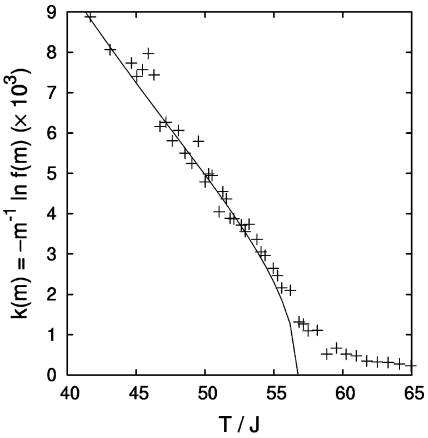

Figure 7. Numerical values for the fitting parameter k in the function $f'(m) = \exp(-km - k_2\sqrt{m})$ fitted as in Figure 6 as a function of dimensionless temperature. The line in the fit is as shown in Figure 4, after substitution of $\alpha = 0.521$.

interaction is short-ranged. This is also the case in the familiar 3D Ising model. A subtle issue is that in our simulations the molar mass distribution is kept constant; this could give rise to so-called "hidden variables" in the context of Fisher renormalization.[46,47] If this is indeed the case, the specific heat takes large values but does not diverge to infinity at the critical point. Consequently, the corresponding critical exponent α'_c is zero, and the other exponents take slightly different values; in particular $\beta' = \beta/(1 - \alpha_c) \approx 0.37$, instead of $\beta = 0.3269$ in the pure Ising model.[48]

In the Ising model, if the critical temperature is approached from below, the magnetization M decreases to zero as $M \sim (T_c - T)^\beta$. In our model, the equivalent of the magnetization is the normalized density difference $|(\rho_A - \rho_B)/(\rho_A + \rho_B)|$. This quantity, raised to the power $1/\beta$, is thus expected to decrease linearly to zero at the critical temperature. The inset of Figure 5 shows this approach for $\beta = 0.3269$ as in the Ising model, $\beta = 0.37$ as expected if Fisher renormalization occurs, and the mean-field value $\beta = 0.5$. Mean-field behavior is inconsistent with our data, but we cannot establish whether Fisher renormalization takes place within our numerical accuracy.

The degree of fractionation of the polymers in the computer simulations shows exponential dependence on the polymer length for long polymers in the simulation. The short polymers deviate slightly due to end group effects: a polymer of length $m > 1$ has less surface than m times that of one monomer. This finite-length effect can be accounted for with $f'(m) \sim \exp(-km - k_2\sqrt{m})$. In Figure 6 the measured values for $f(m)$ are plotted as a function of m. In the same figure, curves for $f'(m)$ with fitted values for k and k_2 are shown as well. The long-polymer limit is retrieved by setting k_2 to zero; in this limit, $k = -m^{-1} \ln f(m)$ is independent of polymer length m. Figure 7 shows the values of k as a function of temperature. A comparison of Figure 4 with Figure 7 shows quantitative agreement well below the critical temperature if $\alpha = 0.521$. Close to the critical temperature we do not expect quantitative agreement due to the finite simulation cell. The value of α describes the combined effect of the stored length of the polymers, which decreases the number of interactions, and the effective coordination z_{eff}, which is smaller than the lattice coordination number z because of shielding of monomers due to neighbors along the chain. Both contributions are insensitive to small temperature changes.

VI. Concluding Remarks

In summary, we discussed the experimental result that fractionation is an exponential function of the molar mass: $f(m) \sim \exp(-km)$. We showed that this scaling is supported by Flory–Huggins theory and computer simulations. Second, we studied the exponent β, which describes the behavior of phase separation as a function of temperature close to its critical value. Within Flory–Huggins theory, this exponent was found to be $\beta_{FH} = 0.5$, consistent with the mean-field estimation of the exponent β in the 3D Ising model, as expected. Within computer simulations, on the other hand, this exponent was found to be consistent with non-mean-field values $\beta = 0.3269$ as found in simulations of the 3D Ising model, as well as $\beta = 0.37$, the Fisher-renormalized critical exponent.

Acknowledgment. We thank the referees for raising the issue of Fisher renormalization and pointing us to refs 24, 25, 46, and 47.

References and Notes

(1) Flory, P. J. *J. Chem. Phys.* **1942**, *10*, 51.
(2) Flory, P. J. *J. Chem. Phys* **1944**, *12*, 425.
(3) Huggins, M. L. *Ann. N.Y. Acad. Sci.* **1942**, *43*, 1.
(4) Huggins, M. L. *J. Am. Chem. Soc.* **1942**, *64*, 1712.
(5) Scott, R. L.; Magat, M. *J. Chem. Phys.* **1945**, *13*, 172.
(6) Scott, R. L. *J. Chem. Phys.* **1945**, *13*, 178.
(7) Scott, R. L. *J. Chem. Phys.* **1949**, *17*, 279.
(8) Hillert, M. *Acta Metall.* **1961**, *9*, 525.
(9) Cahn, J. W. *Acta Metall.* **1961**, *9*, 795.
(10) Cahn, J. W. *Trans. Metall. Soc. AIME* **1968**, *282*, 166.
(11) Hilliard, J. E. In *Phase Transformations*; Arenson, H. I., Ed.; American Society for Metals: Metals Park, OH, 1970.
(12) Langer, J. S.; Bar-on, M.; Miller, M. D. *Phys. Rev. A* **1975**, *11*, 1417.
(13) Binder, K. *Phys. Rev. B* **1977**, *15*, 4425.
(14) Koningsveld, R.; Chermin, H. A. G.; Gordon, M. *Proc. R. Soc. London A* **1970**, *319*, 331.
(15) Helfand, E.; Tagami, Y. *J. Chem. Phys.* **1972**, *56*, 3592.
(16) Koningsveld, R.; Kleintjens, L. A.; Schoffelers, H. M. *Pure Appl. Chem.* **1974**, *39*, 1.
(17) de Gennes, P. G. *J. Chem. Phys.* **1980**, *72*, 4756.
(18) Pincus, P. *J. Chem. Phys.* **1981**, *75*, 1996.
(19) Bergfeldt, K.; Piculell, L.; Linse, P. *J. Phys. Chem.* **1996**, *100*, 3680.
(20) de Sousa, H. C.; Rebelo, L. P. N. *J. Polym. Sci., Part B: Polym. Phys.* **2000**, *38*, 632.
(21) Clarke, N. *Eur. Phys. J. E* **2001**, *4*, 327.
(22) Reister, E.; Müller, M.; Binder, K. *Phys. Rev. E* **2001**, *64*, 041804.
(23) Pagonabarraga, I.; Cates, M. E. *Europhys. Lett.* **2001**, *55*, 348.
(24) Yang, J.; Sun, Z.; Jiang, W.; An, L. *J. Phys. Chem. B* **2002**, *106*, 11305.
(25) Sollich, P. *J. Phys.: Condens. Matter* **2002**, *14*, R79.
(26) Kwei, T. K.; Nishi, T.; Roberts, R. F. *Macromolecules* **1974**, *7*, 669.
(27) Bates, F. S.; Dierker, S. B.; Wignal, G. D. *Macromolecules* **1986**, *19*, 1938.
(28) Kyu, T.; Saldanha, J. M. *Macromolecules* **1988**, *21*, 1021.
(29) Tsai, F.-J.; Torkelson, J. M. *Macromolecules* **1988**, *21*, 1026.
(30) Bates, F. S.; Fettes, L. J.; Wignall, G. D. *Macromolecules* **1988**, *21*, 1086.
(31) Bates, F. S.; Wiltzius, P. *J. Chem. Phys.* **1989**, *91*, 3258.
(32) Edelman, M. W.; Tromp, R. H.; van der Linden, E. *Phys. Rev. E* **2003**, *67*, 021404.
(33) Verdier, P. H.; Stockmayer, W. H. *J. Chem. Phys.* **1962**, *36*, 227.
(34) Evans, K. E.; Edwards, S. F. *J. Chem. Soc., Faraday Trans. 2* **1981**, *77*, 1891.
(35) Deutsch, J. M. *Phys. Rev. Lett.* **1982**, *49*, 926.
(36) Kremer, K. *Phys. Rev. Lett.* **1983**, *51*, 1923.
(37) Deutsch, J. M. *Phys. Rev. Lett.* **1983**, *51*, 1924.
(38) Kolinski, A.; Skolnick, J.; Yaris, R. *J. Chem. Phys.* **1987**, *86*, 7164.
(39) Kolinski, A.; Skolnick, J.; Yaris, R. *J. Chem. Phys.* **1987**, *86*, 7174.
(40) Deutch, H. P.; Binder, K. *J. Chem. Phys.* **1991**, *94*, 2294.
(41) Paul, W.; Binder, K.; Heermann, D. W.; Kremer, K. *J. Chem. Phys.* **1991**, *95*, 7726.
(42) Müller, M.; Wilding, N. B. *Phys. Rev. E* **1995**, *51*, 2079.
(43) Edelman, M. W.; van der Linden, E.; de Hoog, E. H. A.; Tromp, R. H. *Biomacromolecules* **2001**, *2*, 1148.
(44) Newman, M. E. J.; Barkema, G. T. *Monte Carlo Methods in Statistical Physics*; Clarendon Press: Oxford, 1999.
(45) Metropolis, N.; Rosenbluth, A. W.; Rosenbluth, M. N.; Teller, A. H.; Teller, E. *J. Chem. Phys.* **1953**, *21*, 1087.
(46) Fisher, M. E. *Phys. Rev.* **1968**, *176*, 257.
(47) Bergman, D.; Halperin, D. *Phys. Rev. B* **1976**, *13*, 2145.
(48) Talapov, A. L.; Blöte, H. W. J. *J. Phys. A* **1996**, *29*, 5727.
(49) The CPU times have been measured on an alpha EV6.7 (21264A) machine operating at 667 MHz.

MA025736Q